Three-Dimensional Table-Driven Migration

Gerrit Blacquière, Delft University of Technology; Harry W. J. Debeye, Jason Geosystems BV; C. P. A. Wapenaar, and A. J. Berkhout, Delft University of Technology, Netherlands

SUMMARY

A full 3–D wave field extrapolation technique is presented. It can be used for any type of subsurface structure, both with lateral and vertical velocity variations.
The extrapolation is performed recursively in the space-frequency (x-y-ω) domain with precalculated recursive Kirchhoff extrapolation operators, that have been stored in a table.
At the basis of the operator computation is the well-known phase-shift operator. Although this operator is exact for homogeneous layers only, it is assumed that it may be applied locally in case of lateral inhomogeneties. Lateral velocity variations can then be handled by choosing the extrapolation operator according to the local value of the wavenumber, ω/c.
The operators can be designed such that they act as spatially variant high-cut filters. This option means that the evanescent field can be suppressed simultaneously with the extrapolation.
The extrapolation method can be used both in prestack and poststack applications. We used it in zero-offset migration. Tests on synthetic and real data show the high quality of the method.
The implementation yields a code that is vectorizable, which makes the method very suitable for vector computers.

INTRODUCTION

Many current 3–D migration techniques are only approximately valid in case of inhomogeneous media, e.g., 3–D time migration, two-pass depth migration and 3–D depth migration based on operator splitting. If strong velocity variations occur in the subsurface, a *one-pass, true 3-D, depth* migration method should be used, (Yilmaz et al.,1987).
The quality of such a method is determined by the wave field extrapolation. To be able to handle the lateral velocity variations correctly, we perform the extrapolation in the x–y–ω domain (Berkhout, 1982, 1984). Vertical velocity variations are taken into account by dividing the model into small layers and by performing the extrapolation recursively from one depth level to the next.
Some practical problems that have to be avoided in wave field extrapolation are: instability, inaccuracy, poor performance if steep dips are present and spatial operator aliasing.
In this paper we discuss a 3–D table-driven extrapolation scheme in which these problems have been solved. We design the extrapolation operators via the wavenumber-frequency (k_x-k_y-ω) domain. In this way we have control over accuracy and dip-angle performance; optionally it is possible to use the operators also for space-dependent high-angle and evanescent field suppression.
Full 3–D wave field extrapolation is expensive and therefore special attention is paid to the efficiency. We calculate the 3–D extrapolation operators in advance and store them in a table. Also, the symmetry properties of the operators are used to reduce the number of calculations.
We applied this wave field extrapolation method in a 3–D zo-migration scheme.

WAVE FIELD EXTRAPOLATION THEORY

3–D Downward wave field extrapolation, from depth level z_i to depth level $z_{i+1} = z_i+\Delta z$, can be formulated in the x-y-ω domain as:

$$P(x,y,z_{i+1},\omega) = F[x,y,\Delta z,k(x,y,z_i,\omega)] * P(x,y,z_i,\omega), \qquad (1)$$

with:

$$k(x,y,z_i,\omega) = \omega/c(x,y,z_i),$$

P denotes the temporal Fourier transform of the upgoing pressure field,
F denotes the inverse wave field extrapolation operator,
k is the local wavenumber,
c is the propagation velocity of the medium and
the symbol ∗ denotes a two-dimensional space-dependent spatial convolution along the x- and y-coordinates.

The extrapolation according to equation (1) should be applied recursively for all depth levels of interest. This way vertical velocity variations can be taken into account.
Both the quality and the efficiency of the extrapolation are determined by recursive operator F. The expression for F in the k_x-k_y-ω domain is the well known phase-shift operator:

$$\tilde{F}(k_x,k_y,\Delta z,k) = \exp(\sqrt{k^2-k_x^2-k_y^2}\,\Delta z), \text{ for } k^2 \ge k_x^2 + k_y^2, \text{ and}$$
$$\tilde{F}(k_x,k_y,\Delta z,k) = \exp(-\sqrt{k_x^2+k_y^2-k^2}\,\Delta z), \text{ for } k^2 < k_x^2 + k_y^2. \qquad (2)$$

The symbol ~ denotes a spatial Fourier transform. To get short operators in the space domain, first $\tilde{F}$ is modified such that both phase and amplitude become smooth functions (no dis-

continuous first derivatives at $k^2 = k_x^2 + k_y^2$). Optionally a spatial high-cut filter is applied to suppress high dip-angle/evanescent waves. Then it is inverse Fourier transformed to the x-y-ω domain where it is ready to be applied.
The operator can be further optimized by an iterative procedure as introduced by Holberg (1988) for the 2–D case and adapted by Debeye (1988) for the 3–D case.

OPERATOR TABLE

Calculation of the operators during the extrapolation would slow down the speed of the algorithm. Also, each operator is likely to be used many times, either within one migration process, due to the recursive character of the extrapolation, or in other migration processes. Therefore, the operators are calculated in advance and stored in a table for a range of wavenumber values:

$$k_{min}, k_{min}+\Delta k, \ldots, k_{max}-\Delta k, k_{max}.$$

During the extrapolation, the local value of the wavenumber, $k = \omega/c(x,y,z_i)$, is determined after which the appropriate operator is selected from the table and applied to the data.
A disadvantage of an operator table is that an actually required operator is not likely to be present. A solution is to compute the required operators by interpolation. We found that in general linear interpolation of real and imaginary parts gives good results if Δk is in the order of $\Delta\omega/(2c_{max})$.

EXTRAPOLATION IN ZERO-OFFSET MIGRATION

We used the wave field extrapolation method as the basis for a zero-offset depth migration algorithm; it consists of the following two steps:

1. Downward extrapolation, according to:

$$P_{zo}(x,y,z_{i+1},\omega) = F[x,y,\Delta z,2k(x,y,z_i,\omega)] * P_{zo}(x,y,z_i,\omega). \quad (3)$$

P_{zo} denotes the temporal Fourier transform of the upgoing pressure field (zo-data),

Note that equation (3) is the same as equation (1) except for the so-called half velocity substitution (wavenumber k replaced by 2k, 'exploding reflector' assumption).

2. Imaging by integrating over all frequency components of the frequency band of interest. This yields an estimate of the zo-reflectivity (t = 0), according to:

$$\langle R_{zo}(x,y,z_{i+1})\rangle = \frac{1}{\pi}\,\mathrm{Re}\int_{\omega} G(z_{i+1},\omega)\, P_{zo}(x,y,z_{i+1},\omega)\, d\omega. \quad (4)$$

$\langle R_{zo}\rangle$ denotes the band-limited estimate of the zo-reflectivity,
G is an optional weighting function. It can be used for depth variant spectral shaping, e.g., to compensate for absorption or to suppress coherent noise.

These two steps should be applied recursively for all depth levels of interest. The procedure is visualized in Figure 1.

COMPUTATIONAL ASPECTS

In 3–D zo-migration large amounts of data are involved. Therefore it is important to pay attention to the computational aspects. The discretized version of equation (3) is:

$$P_{zo}(q\Delta x,r\Delta y,z_{i+1},\omega) \approx \sum_{m=-M}^{M}\sum_{n=-N}^{N} \langle F[m\Delta x,n\Delta y,\Delta z, 2k(q\Delta x,r\Delta y,z_i,\omega)]\rangle \; P_{zo}[(q-m)\Delta x,(r-n)\Delta y,z_i,\omega]\, \Delta x\Delta y. \quad (5)$$

q=1,numx,
r=1,numy,
numx denotes the number of traces in the x-direction,
numy denotes the number of traces in the y-direction.
the operator size is (2M+1)(2N+1).

One complex addition is equivalent to two real additions, and one complex multiplication is equivalent to four real multiplications and two real additions.
Using this we can express the total number of floating point operations per monochromatic extrapolation step as:

$$8(numx)(numy)(2M+1)(2N+1) \text{ fp-operations.} \quad (6)$$

For the total migration scheme, we must multiply this result by the number of frequency components and by the number of extrapolation steps (we neglect the operator interpolation and the imaging step):

8(numf)(numz)(numx)(numy)(2M+1)(2N+1) fp-operations. (7)

numf denotes the number of frequency components,
numz denotes the number of extrapolation steps.

A result like this must be interpreted with care. Only together with information about the computer power and its architecture (scalar ⇔ vector, parallel processing, add multiply overlap etc.) a good estimate of the performance is possible.

A reduction of the number of fp-operations of about 70% (!) can be reached by using the fact that F is symmetric:

$$F(x,y) = F(-x,y) = F(x,-y). \quad (8)$$

Our method is very well suited for implementation on a vector computer. Working per frequency component offers a natural way of dividing the problem into independent parts for parallel processing. These properties may contribute to an increased efficiency. This is very important because the extrapolation almost completely determines the speed of the migration algorithm.

EXAMPLE / RESULTS

To test the migration algorithm, synthetic exploding reflector data were generated. The subsurface model, shown in Figure 2, consists of a horizontal square part of a reflector below a dipping interface. In this model both lateral and vertical velocity variations are present. A time slice and a vertical cross section of the zo-response (only modeled for the reflector) are shown in Figure 3 and 4. A depth slice and a vertical cross section of the migrated result can be seen in Figure 5 and 6 respectively. Notice the good positioning of the horizontal reflector. Also the diffraction energy is focused well.
Some parameters: temporal sampling interval $\Delta t = 4$ ms, frequency contents $f_{min}=20$ Hz., $f_{max}=80$ Hz., number of frequency components numf=32, velocity $c_{min}=2400$ m/s and $c_{max}=3200$ m/s , grid size 128x128x100 (numx,numy,numz), horizontal grid spacing $\Delta x=7.5$ m and $\Delta y=7.5$ m, vertical grid spacing $\Delta z=5$ m, number of operator points 25 x 25 (M = 12, N = 12), maximum angles of propagation used in the operator design $\alpha_{x,max}=45°$ and $\alpha_{y,max}=45°$, number of operators 137 (in the range from $k_{min}=0.077\,m^{-1}$ to $k_{max}=0.424\,m^{-1}$).
For this configuration the program required 3 hours user time at a rate of 8.2 Mflop on a Convex C1–XP.
More examples will be discussed during the presentation.

CONCLUSIONS

3–D Table-driven wave field extrapolation can be a powerful tool in many seismic applications. We discussed the recursive use of the extrapolation in zo-migration.
The example shows that the method can handle both lateral and vertical velocity variations: the reflectivity is positioned well and diffraction energy is focussed correctly.
A good efficiency has been reached by using precalculated (optimized) operators in a table and by using the symmetry properties of the operators.
The method is very well suited for vector computers. A parallel implementation can be realized in a natural way, because the frequency components are treated independently. These properties may also contribute to an increased efficiency.

ACKNOWLEDGMENTS

The investigations were supported by the sponsors of the TRITON consortium project at the Laboratory of Seismics and Acoustics of the Delft University, The Netherlands.

REFERENCES

Yilmaz, O., Chambers, R., Nichols, D., and Abma, R., 1987, Fundamentals of 3–D migration: Geophysics: The leading edge of exploration, **6**, 22-30, and **7**, 26-33.

Holberg, O., 1988, Towards optimum one-way wave propagation: Geophysical prospecting, **36**, 99-114.

Debeye, H.W.J., 1988, Optimization of the recursive Kirchhoff operator: Master's thesis, Laboratory of Seismics and Acoustics, Delft University of Technology.

Berkhout, A.J., 1982, Seismic migration: Imaging of acoustic energy by wave field extrapolation. A. Theoretical aspects: Elsevier Science Publ. Co., Inc.

Berkhout, A.J., 1984, Seismic migration: Imaging of acoustic energy by wave field extrapolation. B. Practical aspects: Elsevier Science Publ. Co., Inc.

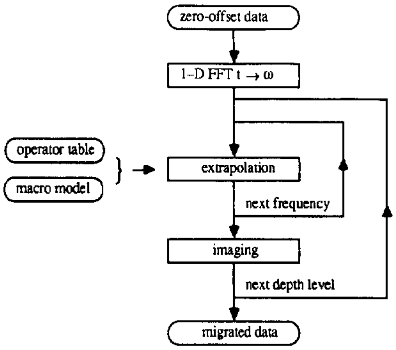

FIG. 1. Flow chart of 3-D zero-offset migration scheme.

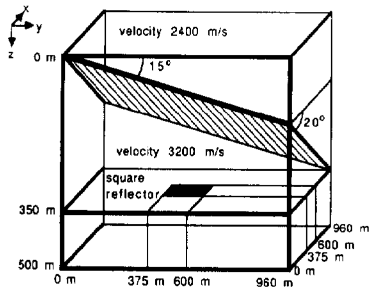

FIG. 2. Subsurface model used in generation of zero-offset data. Only response of square reflector was modeled.

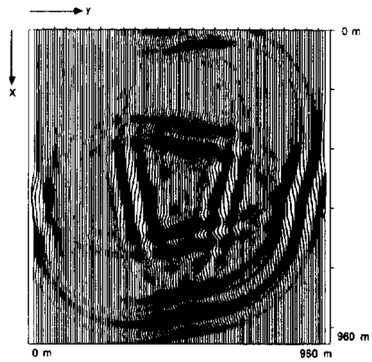

FIG. 3. Zero-offset response of square reflector, time slice, $t = 0.36$ s.

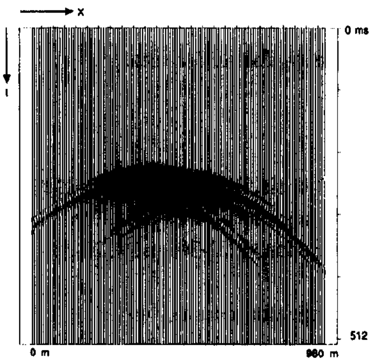

FIG. 4. Zero-offset response of square reflector, x, t-panel, $y = 480$ m.

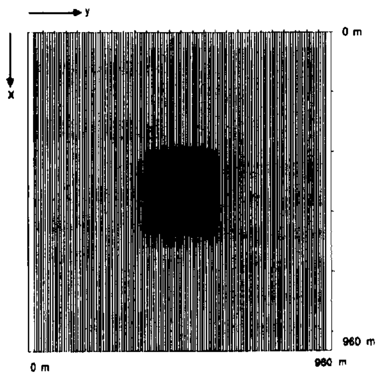

FIG. 5. Table-driven migrated result, depth slice, $z = 350$ m.

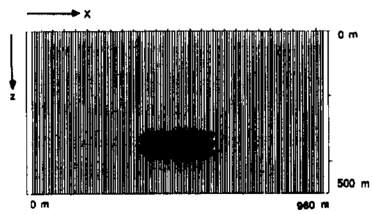

FIG. 6. Table-driven migrated result, x, z-panel, $y = 480$ m.